Resistive switching effect in $SrTiO_{3-\delta}$/Nb-doped $SrTiO_3$ heterojunction

M. C. Ni
Department of Physics, Tsinghua University, Beijing 100084, China and Department of Physics, Changchun University of Science and Technology, Changchun 130022, China

S. M. Guo, H. F. Tian, and Y. G. Zhao[a)]
Department of Physics, Tsinghua University, Beijing 100084, China

J. Q. Li
Beijing National Laboratory for Condensed Matter Physics, Institute of Physics, Chinese Academy of Sciences, Beijing 100080, China

(Received 8 September 2007; accepted 7 October 2007; published online 29 October 2007)

The authors report on the fabrication and properties of $SrTiO_{3-\delta}$/Nb-doped $SrTiO_3$ heterojunctions. The current-voltage curves of these junctions show hysteresis and remarkable resistive switching behavior. Hysteresis was also observed in the capacitance-voltage curves of these junctions. Upon applying voltage pulses, the resistance of the heterojunctions can be switched between different states and the relaxation of the junction current after switching follows the Curie–Von Schweidler law. The results were discussed by considering the role of defects in the interfacial depletion region of the heterojunctions. This work indicates that heterojunctions composed of two oxides can also show the switching effect, which is useful for applications. © *2007 American Institute of Physics*. [DOI: 10.1063/1.2803317]

Recently, the resistive switching effect in the transition metal oxides has attracted much attention due to its importance in both basic research and applications.[1] It has been shown that the current-voltage (*I-V*) curves of heterostructures composed of a metal and a transition metal oxide show hysteresis and electric voltage pulses can switch the heterostructures into different resistance states. Up to now, most of the reports on resistive switching effect are related to heterostructures made of a metal and a transition metal oxide, and the metal electrodes are believed to be important for the switching effect. Recently, however, the resistive switching effect was also observed in $La_{1-x}Sr_xFeO_3/SrTi_{0.99}Nb_{0.01}O_3$ (Ref. 2) and $SrRuO_3/SrTi_{1-x}Nb_xO_3$ (Ref. 3) indicating that heterostuctures composed of two oxides may also be good candidates for exploring the resistive switching effect. Moreover, the study on the capacitance and relaxation of junction current for the resistive switching effect is rather limited. Thus, it is interesting to explore the resistive switching effect in heterostuctures composed of other oxides.

$SrTiO_3$ (STO) is an interesting material, which shows various properties. Considering the tunability of STO, it is interesting to explore if the STO based heterojunctions can show the resistive switching effect. Choi *et al.* studied the polycrystalline $SrTiO_x$ based $Pt/SrTiO_x/Si$ heterostructure and found the resistive switching effect,[4] which was attributed to the $Pt/SrTiO_x$ interface. In this letter, we report the fabrication and property of $SrTiO_{3-\delta}$/Nb-doped $SrTiO_3$ (STO/NSTO) heterojunctions. The *I-V* curves of these junctions show resistive switching phenomena, which originate from the defects at the interface of STO/NSTO. It was also demonstrated that the resistance of the heterojunctions can be switched between different states by applying short voltage pulses, manifesting its significance in applications.

STO thin film was deposited on the (100) oriented, 0.7 wt % Nb-doped $SrTiO_3$ (NSTO-7) substrate using the pulsed laser deposition. A STO single crystal was used as the target. The laser pulse frequency was 5 Hz, and the pulse energy density was about 1.5 J/cm^2. During the deposition process, a substrate temperature of 650 °C and an oxygen pressure of 13 Pa were maintained. After deposition, the film was cooled down to room temperature at 0.5 atm of oxygen pressure. The thickness of STO film is about 150 nm. This heterojunction is denoted as STO/NSTO-7. For comparison, STO thin film was also deposited on the (100) oriented, 0.1 wt % Nb-doped $SrTiO_3$ (NSTO-1) substrate, and this heterojunction is named as STO/NSTO-1. Gold was deposited as top electrode by magnetron sputtering using a shadow mask. Indium was pressed on the back of NSTO substrate as the bottom electrode. The θ-2θ x-ray diffraction patterns of the junction, obtained by using a Rigaku diffractometer with Cu K_α radiation, do not show impurity peaks. A Tecnai-F20 (200 kV) transmission electron microscope (TEM) was used for the microstructure analysis. The current-voltage (*I-V*) curves of the junction were measured by a two-probe method [inset of Fig. 1(a)] with a Keithley 2400 source meter. In order to protect the samples, a compliance current of 10 mA was used. A pulsed dc voltage with a width of 0.5 s and an interval of 2 s was applied to measure the *I-V* curves. The capacitance of the junction was measured by a *LCR* meter ZM2353.

Figures 1(a) and 1(b) are the *I-V* curves of STO/NSTO-7 at different temperatures. Besides the rectifying behavior, this junction also shows a remarkable resistive switching behavior and the resultant hysteresis. The hysteresis decreases with the decrease of temperature. In order to get some clues to the origin of resistive switching behavior, we also measured the *I-V* curves of STO/NSTO-1 at different temperatures and they do not show obvious resistive switching behavior (not shown). The results for STO/NSTO-1 and STO/NSTO-7 were repeated on other samples. The comparison between the *I-V* curves of STO/NSTO-7 and those of STO/NSTO-1 suggests that the resistive switching behavior

a)Electronic mail: ygzhao@tsinghua.edu.cn

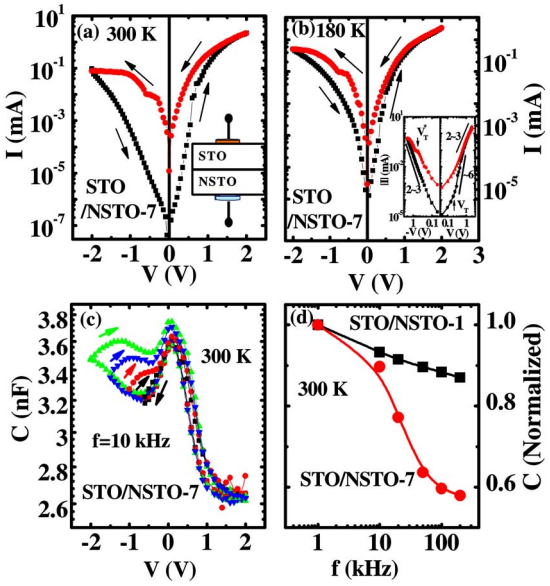

FIG. 1. (Color online) *I-V* curves of the STO/NSTO-7 heterojunction at (a) 300 K and (b) 180 K. The arrows indicate the bias voltage sweeping direction. The inset of (a) shows the schematic of the junction and electrode setting. The inset of (b) illustrates the log-log plots for the *I-V* curve of STO/NSTO-7 at 180 K. The straight lines are guides for the eye. (c) The *C-V* curves for STO/NSTO-7 with different maximum negative sweeping voltages (−2, −1.5, −1, and −0.6 V). The arrows indicate the bias voltage sweeping direction. (d) Frequency dependence of capacitance for STO/NSTO-1 and STO/NSTO-7, respectively.

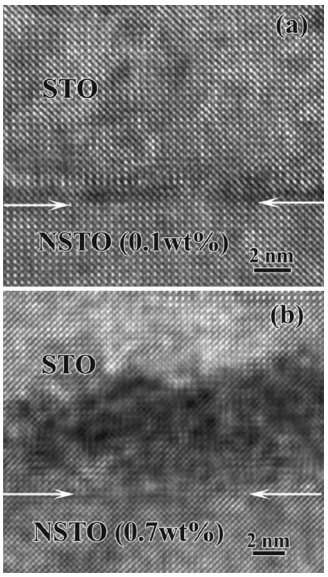

FIG. 2. High-resolution TEM images obtained from cross-sections of (a) STO/NSTO-1 (b) STO/NSTO-7.

and the resultant hysteresis in STO/NSTO-7 are related to the interface of STO/NSTO-7.

We also measured the capacitance of STO/NSTO-1 and STO/NSTO-7. The capacitance-voltage (*C-V*) curves for STO/NSTO-7 measured with different maximum negative sweep voltages also show hysteresis, as shown in Fig. 1(c). Threshold voltage for the appearance of *C-V* hysteresis is about −0.6 V for the negative bias. For STO/NSTO-1, however, the *C-V* curve does not show hysteresis (not shown). Figure 1(d) is the frequency dependence of capacitance for STO/NSTO-1 and STO/NSTO-7. It can be seen that the capacitance of STO/NSTO-7 decreases with the increasing frequency and shows remarkable frequency dependence, while the capacitance of STO/NSTO-1 shows small decrease with the increasing frequency. Fukuda *et al.* studied the frequency dependence of capacitance of $Pt/Ba_{0.5}Sr_{0.5}TiO_3/Pt$ capacitor and they found that the oxygen vacancies in the interfacial depletion region play an important role in determining the property of the capacitor.[5] For sample with more oxygen vacancies, its capacitance decreases with increasing frequency dramatically, in contrast to the insensitivity of capacitance to frequency for sample with much less oxygen vacancies. It is likely that the defects in the interfacial depletion region of STO/NSTO also dominate its behavior, as will be discussed later.

In order to directly demonstrate the different structural features between the STO/NSTO-1 and STO/NSTO-7 samples, a TEM examination on the interfacial regions has been performed for these heterojunctions. Figures 2(a) and 2(b) show the high-resolution TEM images obtained from cross-sections of STO/NSTO-1 and STO/NSTO-7, respectively. It is recognizable that the STO/NSTO-1 heterojunction has a well-matched interface structure in sharp contrast with STO/NSTO-7 which contains notable structural distortions and defects near the interfacial regions. This structural distinction may account for the observed difference in the *I-V* behaviors between these two heterojunctions. It has been reported that Nb stripes are formed for NSTO with high concentration of Nb.[6] This may facilitate the formation of defects at the interface of NSTO-7, whose Nb concentration is higher.

In order to study the temporal variation of the response of STO/NSTO-7 to the voltage pulses, the variation of the junction current for STO/NSTO-7 with a train of voltage pulses of given polarities was measured and the result is shown in Fig. 3. Figure 3(a) is the train of voltage pulses with +2 and −2 V, respectively, and Fig. 3(b) is the response of the heterojunction current to the train of voltage pulses. It

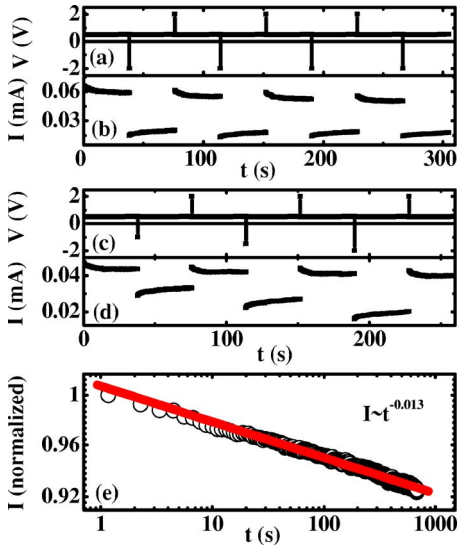

FIG. 3. (Color online) Tunability of the STO/NSTO-7 heterojunction current with a train of voltage pulses of given polarities. (a) The train of voltage pulses with +2 and −2 V. (b) Response of the heterojunction current to the train of voltage pulses shown in (a). (c) The train of voltage pulses with +2 and −1 and −1.5 and −2 V, respectively. (d) Response of the heterojunction current to the train of voltage pulses shown in (c). (e) Relaxation of the STO/NSTO-7 heterojunction current with time after switching due to a positive voltage pulse.

can be seen that the train of voltage pulses can switch the heterojunction between different resistive states with the positive voltage pulses decreasing the resistance (increasing current) and the negative voltage pulses increasing the resistance (decreasing current). The effect of the magnitude of the pulse voltage on the junction current for STO/NSTO-7 was also studied. Figure 3(c) is the train of voltage pulses with +2 and −1 and −1.5 and −2 V, respectively, and the response of the heterojunction current to the train of voltage pulses is shown in Fig. 3(d). Figure 3(e) is the variation of the STO/NSTO-7 heterojunction current with time after switching. It can be seen that it follows the Curie–Von Schweidler law $J \propto t^{-n}$ with $n=0.013$. For Curie–Von Schweidler law, n is positive and smaller than 1 (Ref. 7). The value of n for STO/NSTO-7 is much smaller than that of other materials,[8] whose relaxation current is related to the bulk effect. The junction current relaxation can be understood by the defects near the interface.

NSTO is a degenerate n-type semiconductor while STO film usually contains oxygen vacancies, which act as a donor defect. Thus, a n-n^+ junction is expected to be formed at the STO-NSTO interface, which can account for the rectifying I-V characteristic of the junction. Since the carrier concentration of NSTO is much larger than that of STO, the built-in potential of the junction should be mainly applied to STO. As a result, the depletion layer of STO-NSTO junction is mainly in STO. The property of the junction is determined by the depletion layer. Various models have been proposed to explain the resistive switching effect,[1] such as Schottky barriers with interface states, electrochemical migration at the interface, etc., but the mechanism is still an open question. Based on the experimental results, we can interpret the resistive switching of STO-NSTO-7 junction as a trapping-detrapping process of carriers due to defects in the interfacial depletion region. The inset of Fig. 1(b) shows the log-log plots for the I-V curve of STO/NSTO-7 at 180 K. For the positive bias voltage, the current shows quadratic behavior first, then rises rapidly (slope of ~6) at the critical voltage (V_T) about 0.2 V, and finally increases slowly with slope of 2–3. This behavior can be well described by the trap-controlled space charge limited current (SCLC) mechanism[9] with the three regions corresponding to the trap-unfilled, trap-filled SCLC and trap-free SCLC regimes, respectively. Moreover, V_T is the transition voltage from trap-unfilled to trap-filled SCLC regimes.[10] From 2 to 0 V, the current retains the higher value indicating that the trapped carriers are not released from the trap centers, which result in the hysteresis behavior. From 0 to −2 V, the reverse voltage aids the release of the carriers from the traps and the current increases rapidly until shallow trapped carriers are completely released at the negative critical voltage (V_T^*) of about −0.6 V. With the increase of absolute bias value, the deep trapped carriers are excited and the hysteresis appears due to the long relaxation time for them. The trapping and detrapping of carriers can also lead to the hysteresis of C-V curves as well as the decrease of capacitance with increasing frequency because the relaxation time of the trapped carriers is too long to respond to the high frequency variation.[11] Different types of defects have been reported in STO, such as Ti^{4+} Frenkel defects with Ti^{4+} interstitials, Sr vacancies, etc., which serve as electron traps.[4,12] It is possible that the Nb stripes on NSTO-7 facilitate the formation of defects at the interface of STO-NSTO-7. These defects play a key role in controlling the conduction of electrons at the interface. Therefore, the resistive switching effect may be tuned via defect engineering at the interface of the heterojunctions.

In summary, we have studied I-V characteristics of the STO/NSTO junctions with different Nb doping levels. STO/NSTO-7 shows a remarkable resistive switching behavior and the resultant hysteresis, which are absent in STO/NSTO-1. Hysteresis was also shown in the capacitance-voltage curves. TEM observation shows that the quality of the interface for STO/NSTO-1 is much better than that of STO/NSTO-7. The resistance of the heterojunction can be switched between different states by applying voltage pulses and the relaxation of the junction current after switching follows the Curie–Von Schweidler law. The results were explained by considering the role of defects at the interface of the junction.

We are grateful to C. M. Xiong for helpful discussion. This work was supported by the National Science Foundation of China (Grant Nos. 50425205, 10674079, 50628202, and 50272031) and National 973 projects (Grant Nos. 2006CB921502 and 2002CB613505).

[1] S. Q. Liu, N. J. Wu, and A. Ignatiev, Appl. Phys. Lett. **76**, 2749 (2000); M. Quintero, P. Levy, A. G. Leyva, and M. J. Rozenberg, Phys. Rev. Lett. **98**, 116601 (2007); Y. B. Nian, J. Strozier, N. J. Wu, X. Chen, and A. Ignatiev, *ibid.* **98**, 146403 (2007); C. Rossel, G. I. Meijer, D. Bremaud, and D. Widmer, J. Appl. Phys. **90**, 2892 (2001); M. J. Rozenberg, I. H. Inoue, and M. J. Sanchez, Phys. Rev. Lett. **92**, 178302 (2004); M. Hamaguchi, K. Aoyama, S. Asanuma, and Y. Uesu, Appl. Phys. Lett. **88**, 142508 (2006); D. S. Shang, Q. Wang, L. D. Chen, R. Dong, X. M. Li, and W. Q. Zhang, Phys. Rev. B **73**, 245427 (2006); R. Fors, S. I. Khartsev, and A. M. Grishin, *ibid.* **71**, 045305 (2005).
[2] A. Yamamoto, A. Sawa, H. Akoh, M. Kawasaki, and Y. Tokura, Appl. Phys. Lett. **90**, 112104 (2007).
[3] T. Fujii, M. Kawasaki, A. Sawa, Y. Kawazoe, H. Akoh, and Y. Tokura, Phys. Rev. B **75**, 165101 (2007).
[4] D. Choi, D. Lee, H. Sim, M. Chang, and H. Hwang, Appl. Phys. Lett. **88**, 082904 (2006).
[5] Y. Fukuda, K. Numata, K. Aoki, and A. Nishimura, Jpn. J. Appl. Phys., Part 1 **35**, 5178 (1996).
[6] R. Dittmann, Proceedings of the 13th International Workshop on Oxide Electronics, Ischia, Italy, 2006 (unpublished).
[7] A. K. Jonscher, *Dielectric Relaxation in Solids* (Chelsea, London, 1983).
[8] S.-G. Yoon, A. I. Kingon, and S.-H. Kim, J. Appl. Phys. **88**, 6690 (2000); X. G. Tang, J. Wang, Y. W. Zhang, and H. L. W. Chan, *ibid.* **94**, 5163 (2003).
[9] M. A. Lampert and P. Mark, *Current Injection in Solids* (Academic, New York, 1970).
[10] A. Odagawa, H. Sato, I. H. Inoue, H. Akoh, M. Kawasaki, and Y. Tokura, Phys. Rev. B **70**, 224403 (2004).
[11] M. Yun, R. Ravindran, M. Hossain, S. Gangopadhyay, U. Scherf, T. Bunnagel, F. Galbrecht, M. Arif, and S. Guha, Appl. Phys. Lett. **89**, 013506 (2006).
[12] H. Schmalzried, *Progress in Solid State Chemistry* (Pergamon, New York), Vol. 2, Chap. 8; T. Ohnishi, M. Lippmaa, T. Yamamoto, S. Meguro, and H. Koinumab, Appl. Phys. Lett. **87**, 241919 (2005).